

## Phase Transformation and Stress Distribution in Polished PCD Composites

Yiqing Chen<sup>a</sup> and L.C. Zhang<sup>b</sup>

School of Mechanical and Manufacturing Engineering,  
The University of New South Wales, NSW 2052, Australia

<sup>a</sup>y.chen@unsw.edu.au, <sup>b</sup>Liangchi.Zhang@unsw.edu.au

**Keywords:** Polycrystalline diamond; composites; polishing; dynamic friction; Raman spectrum; phase transformation; residual stress

**Abstract.** With the aid of the Raman spectroscopy, this paper investigates the phase transformation and residual stress distribution in surfaces of polycrystalline diamond composites polished by dynamic friction technique. To clarify the contribution of phase transformations to residual stresses, the study focused on the surface which was incompletely polished such that the transformed phases remained. It was found that amorphous non-diamond carbon and amorphous graphite phase appeared in grain boundaries, but pristine diamond phase was predominant within grain areas. The residual stresses vary across the polished surfaces and the maximum stress locates at the grain boundaries.

### Introduction

Polycrystalline diamond composites (PCDCs) have been widely used as cutting tools due to their ultra high hardness, wear resistance and chemical inertness. However, also because of these properties, the polishing of PCDCs has been very difficult. Moreover, different properties of the PCDC constituents, e.g., diamond and SiC, and the random orientations of the diamond grains in the composites have made the PCDC polishing extremely inefficient by conventional methods. Recently, a cost-effective abrasive-free process, the dynamic friction polishing (DFP) technique [1-8], has been investigated in detail. This technique makes use of the thermo-chemical reaction induced by the frictional heating at the sliding interface between a PCDC specimen and a rotating catalytic metal disk. The previous studies have found that the material removal mechanisms during the dynamic friction polishing involves mainly the following processes: (1) the transformation of the diamond at the PCDC-metal interface to amorphous non-diamond phases due to the interaction with the catalytic metal at an elevated temperature, and (2) the mechanical material removal of the transformed softer amorphous materials by continuous rubbing between the PCDCs and the metal disk. However, the residual phases and stresses in such polished surfaces have not yet been investigated although a deep understanding of these is important to the reliable applications of PCDCs.

The purpose of this research is to investigate the micro-structural changes and obtain a residual stress distribution figure in polished PCDC surface. The Raman spectroscopy will be used to distinguish different forms of carbon and determine the stresses in the material [9-12].

### Experiment

Two types of thermally stable PCDCs were used for the experiment. As shown in Table 1, the Type 1 PCDC contains about 99% of polycrystalline diamond particles in a wide range of grain sizes with an initial surface roughness of  $R_a \approx 4 \mu\text{m}$ . The Type 2 PCDC contains about 70~75% diamond particles of  $\sim 25 \mu\text{m}$  in grain size (the rest are SiC and Si) with an initial surface roughness of  $R_a \approx 1.7 \mu\text{m}$ . A typical specimen was 12.7 mm in diameter and 4 mm in thickness, weighted approximately 1.7 grams.

The polishing experiments were carried out on a machine manufactured in-house, as detailed elsewhere [2], by pressing a PCDC specimen on to a rotating catalytic metal disk in dry atmosphere. The sliding speed between the specimen and the metal disk was 25 m/s, and the polishing pressure used was 3.1 MPa. The polishing time used was 3 minutes. In this case the surfaces would not be completely polished and the transformed phases could remain so that the effect of phase transformations on the residual stresses could be observed.

Table 1 Specifications of the PCDCs used in experiment

	Type 1	Type 2
Diamond percentage (%)	99	70 ~ 75
Grain size of the polycrystalline diamond ( $\mu\text{m}$ )	Non-uniform	~25
Surface roughness Ra ( $\mu\text{m}$ )	4	1.7
Size: diameter (mm) x thickness (mm)	12.7 x 4	12.7 x 4

The surface roughness of polished/unpolished surfaces was measured using SurfTest 402 and SurfTest Analyzer (Mitutoyo). Surface topography including possible micro-cracks was examined by an optical microscope (Leica DM RXE). The surface structure and morphology were also studied using a scanning electron microscope (SEM) FEI Quanta 200 3D, operating at 15 kV.

The Raman spectra were collected using a Renishaw Raman InVia Reflex equipped with a charge-coupled device (CCD) camera. The collection optics was based on a Leica DMLM microscope. The zones for the recording of spectra were selected optically, and they were excited by an argon 514.5 nm laser. The spectra were obtained by using a microscope objective lens (x 50) to focus the incident power (at 2 mW) onto the PCDC surface with a spot size of about 1  $\mu\text{m}$ . Daily calibration of the wave-number axis is required and was achieved by recording the Raman spectrum of silicon (one accumulation, 10s) for both static and extended modes. The spectrometer was controlled by a PC with instrument-control software (Renishaw WiRE 2.0 service pack 9).

Maps were generated by collecting the Raman spectra from areas of  $\sim 50 \mu\text{m} \times 50 \mu\text{m}$  from a PCDC sample with the step size of 4  $\mu\text{m}$ . The spectral acquisition parameters were as follows: static mode, grating position centered at  $1300 \text{ cm}^{-1}$ , 2 scan, 5 seconds exposure, X 50 objective. The laser power at the sample was  $\sim 5 \text{ mW}$ . A representative spectrum from the map dataset was curve fitted using the initial parameter Gaussian-Lorentzian mixture and the resultant curve-fitting parameters were saved. A map of the band position was then produced by fitting the individual spectra within the map dataset using the previously saved parameters.

## Results and Discussion

Diamond peaks shifted from  $1332 \text{ cm}^{-1}$  are evidence of residual stresses. Up-shift of the Raman peak is caused by compression while a downshift is caused by tension. The Raman shift is known to be proportional to the stress in the PCDCs, and the stress can be estimated as [9, 13-14].

$$\sigma = -0.567 (\omega_m - \omega_0) \quad (1)$$

where  $\omega_0 = 1332 \text{ cm}^{-1}$  corresponds to stress-free state of diamond, and  $\omega_m$  is the measured Raman peak position.

The Type 1 PCDC samples used for polishing tests were as-sintered. These PCDCs could not be processed by electrical discharge machining (EDM) as they are mainly made of diamond ( $\sim 99\%$ ) and are not electrically conductive. Raman spectra peak at  $1332 \text{ cm}^{-1}$  predominate most of the collected spectra, indicating that the surfaces were stress-free before polishing.

The Type 2 PCDCs contain sufficient silicon carbide bond which is electrically conductive. Thus EDM was used to obtain desired sample dimensions. As a result, the sample surfaces before polishing had been reduced to  $Ra \approx 1.7 \mu\text{m}$ . The Raman spectra of these PCDCs had a sharp intense diamond peak at  $1333 \text{ cm}^{-1}$ , which, according to Eq. (1), means that the initial surface stresses

before polishing was approximately  $-0.567$  GPa. The spectra also showed a broad band of amorphous graphite at  $1585\text{ cm}^{-1}$ , a heavily disorder band of SiC at  $799\text{ cm}^{-1}$  and a small silicon peak at  $521\text{ cm}^{-1}$ , respectively. On different spots of a PCDC surface, the relative intensities of diamond, SiC, or Si band were found to be different. This indicates that these material phases distributed across the samples unevenly.

After polishing, the surface roughness of Type 1 PCDCs reduced to  $R_a \approx 0.5\text{ }\mu\text{m}$  from its initial  $4\text{ }\mu\text{m}$  without cracking. Under the same polishing conditions, the surface roughness of Type 2 PCDCs became  $R_a \approx 0.2\text{ }\mu\text{m}$ , but cracking occurred.

Raman analysis was performed on both types of the polished specimens. Figure 1 shows some typical Raman spectra of the Type 1 PCDCs. The fingerprint of diamond peak at around  $1332\text{ cm}^{-1}$  was predominant with the diamond grain areas of the polished surfaces, while at the grain boundaries other peaks corresponding to the transformed  $sp^2$ -bonded carbon phases were also found in many spectra. Theoretically, diamond may be transformed to other amorphous non-diamond carbon in addition to graphite or amorphous graphite. This can be approved by the fact that broad bands of amorphous graphite at  $1580\text{--}1590\text{ cm}^{-1}$  and amorphous non-diamond carbon around  $1328\text{--}1336\text{ cm}^{-1}$  were observed in areas of the grain boundaries. Some spectra exhibited two phases at one spot. At the edge of a diamond grain, some diamond peak splits into a higher frequency one and a lower frequency one at a low density. Large variations in the Raman line shapes and positions across a polished surface were observed. The amorphous carbon band was displayed in the form of asymmetric broadening, shift, and splitting of the line.

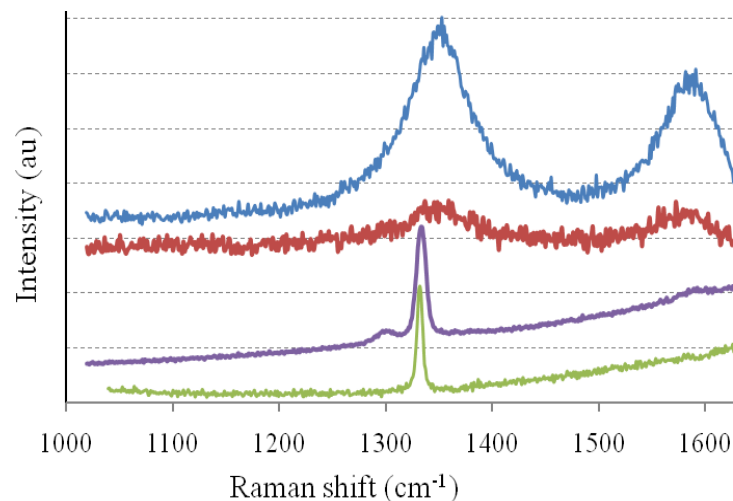


Fig. 1 Typical Raman spectra and its distribution.

Figure 2 shows the surface maps generated from the collected Raman spectra: intensity of the diamond line at  $1332\text{ cm}^{-1}$ , intensity of the amorphous graphite line at  $1588\text{ cm}^{-1}$ , and stress map as a function of position, as calculated from formulae (1). A complex picture has been observed within the map, but some general tendency in the stress distribution can be still traced. The distributions of the phases and stresses on the surface appear to be non-uniform across most areas. Peaks of amorphous diamond and graphite phases were more strongly pronounced on grain boundaries. This was probably due to the constraint of a non-transformed diamond grain that supported high residual stress on the surface. The maximum stress appears at grain boundaries, accompanied by the polishing-induced phase of amorphous non-diamond carbon around  $1328\text{--}1336\text{ cm}^{-1}$ . An estimation of the maximum stress magnitude, according to Eq. (1), gives a value of  $\pm 2.3$  GPa for the surfaces mapped. One of the sources of the high stresses can be the non-uniform distribution of the transformed phases in the polished surface.

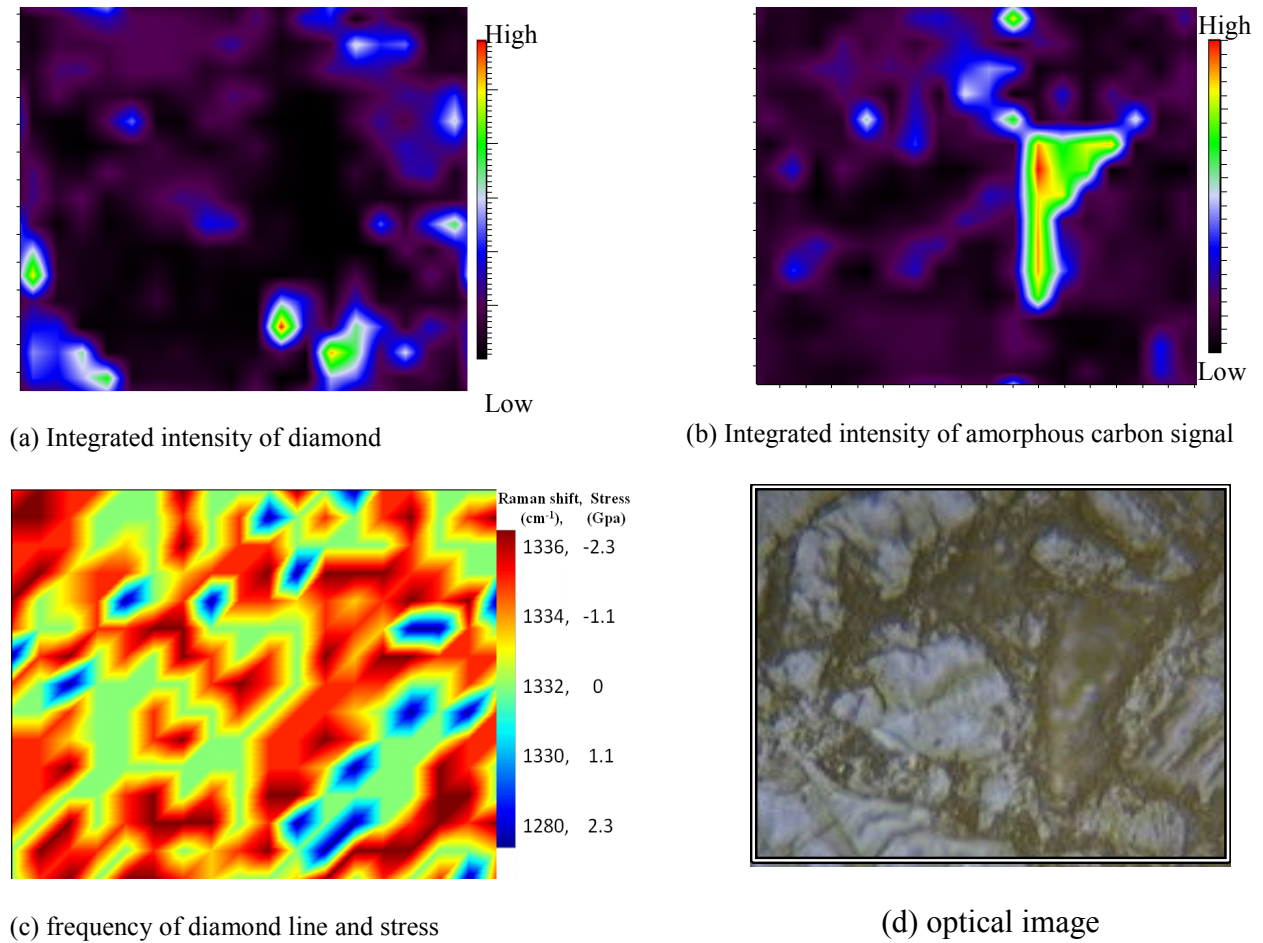


Fig. 2 Raman map of polished Type 1 PCDC

Figure 3 shows the macro Raman spectrum which was obtained by averaging the 270 spectra used to generate the images in Fig. 2. Although the average frequency ( $1332\text{ cm}^{-1}$ ) indicates that the stress in the mapping area is approximately zero, it does not necessarily mean that there is not a high local stress. Moreover, the high intensity of the diamond peak indicates that the quantities of the non-diamond phases are very small.

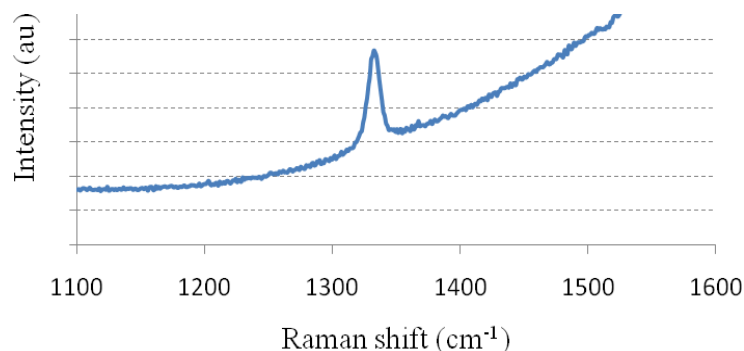


Fig. 3 Macro- Raman (averaging) spectrum of the polished Type 1 PCDC

After polishing under the above conditions, the surface roughness of the Type 2 PCDCs became  $R_a \approx 0.2\ \mu\text{m}$  which is better than that of the Type 1 PCDC surfaces of about  $0.5\ \mu\text{m}$ . However, cracking was found on the surfaces. Such cracking was attributed to the non-uniform thermal stresses in the PCDCs due to the mismatch of thermal expansion coefficients of diamond and silicon carbide. When the polishing temperature increases at a high speed-pressure combination, the

thermal stresses increase to a great enough level, causing cracks to form and extend along the PCD-SiC boundaries.

On the other hand, since Type 1 PCDCs are made of a very high percentage of diamond, the thermal stresses caused by the mismatch of thermal expansion coefficients were negligible, leading to crack-free samples under the conditions tested.

Some selected typical Raman spectra from a polished Type 2 PCDC surface with cracks are shown in Fig. 4. The spectra in grain and boundary regions are quite distinct. At a spot with a grain (e.g., Region A), the spectrum contains a hardly detected SiC band at  $799\text{ cm}^{-1}$ , very weak Si peak at  $\sim 522\text{ cm}^{-1}$  and a high intensity of diamond peak at  $\sim 1332\text{ cm}^{-1}$ , indicating a stress free or low stress state. At the spots near the crystal edge (e.g., Region B), there was a low intensity of Si band and diamond line at  $1334\text{ cm}^{-1}$ . The magnitude of the stress is estimated to be  $-1.314\text{ GPa}$ . The cracked area (e.g., Region C) had a very low intensity of diamond peak at  $\sim 1332\text{ cm}^{-1}$ , weak amorphous graphite band at  $\sim 1580\text{ cm}^{-1}$ , deformed/amorphous SiC band centre at  $\sim 799\text{ cm}^{-1}$  and a high intensity of Si peak at  $\sim 522\text{ cm}^{-1}$ . The cracking should have released the stresses in this region. At grain boundaries (e.g., Region D), the spectra are dominated by the  $sp^2$ -bonded amorphous carbon at  $\sim 1320$ - $1350$  and  $\sim 1580$ - $1590\text{ cm}^{-1}$ .

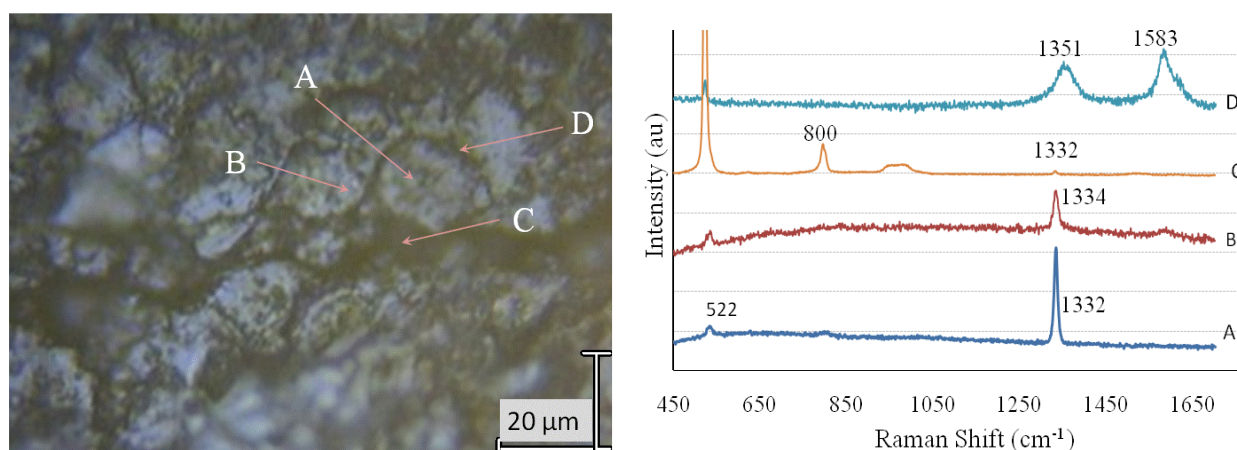


Fig. 4 Polished Type 2 PCDC surface with a crack and the typical Raman spectra.

From the above analysis, it can be seen that stresses in PCDCs are not uniformly distributed but localized near the crystal edges. Higher values are often observed close to the points of contact between adjoining crystals.

## Conclusions

The Raman spectroscopy has been used to investigate the phase transformation and stress variation in incompletely polished PCDC surfaces. It was found that the pristine diamond phase was predominant in grain areas, while amorphous non-diamond carbon and amorphous graphite appeared in grain boundaries. High local stresses, both compressive and tensile, were developed in small regions near crystal edges and grain boundaries. It may conclude that it was the non-uniformity of the phase transformations that had caused the stress fluctuations. When these polishing-induced phases are removed in the consequent processes, the residual stresses may change. This will be clarified in further investigations.

## Acknowledgements

The authors appreciate the Australian Research Council for their financial support to this research.

---

**References**

- [1] Y. Chen, T. Nguyen and L. C. Zhang: International Journal of Machine Tools and Manufacture, vol. 49 (2009), p. 515
- [2] Y. Chen and L. C. Zhang: International Journal of Machine Tools and Manufacture, vol. 49 (2009), p. 309
- [3] Y. Chen, L. C. Zhang and J. Arsecularatne: International Journal of Machine Tools and Manufacture, vol. 47 (2007), p. 2282
- [4] Y. Chen, L. C. Zhang and J. Arsecularatne: in 8th International Symposium on Measurement Technology and Intelligent Instruments, Sendai, Japan, 2007, p. 351
- [5] Y. Chen, L. C. Zhang and J. Arsecularatne: Key Engineering Materials, vol. 364-366 (2008), p. 226
- [6] Y. Chen, L. C. Zhang and J. A. Arsecularatne: International Journal of Machine Tools and Manufacture, vol. 47 (2007), p. 1615
- [7] Y. Chen, L. C. Zhang and J. A. Arsecularatne: International Journal of Surface Science and Engineering, vol. 1 (2007), p. 360
- [8] Y. Chen, L. C. Zhang, J. A. Arsecularatne and et al.: International Journal of Machine Tools and Manufacture, vol. 46 (2006), p. 580
- [9] W. Fortunato, A. J. Chiquito, J. C. Galzerani and et al.: Journal of Materials Science, vol. 42 (2007), p. 7331
- [10] J. W. Ager and M. D. Drory: Physical Review B, vol. 48 (1993), p. 2601.
- [11] H. Windischmann and K. J. Gray: Diamond and Related Materials, vol. 4 (1995), p. 837
- [12] D. S. Knight and W. B. White: Journal of Materials Research, vol. 4 (1988), p. 385
- [13] V. G. Ralchenko, A. A. Smolin, V. G. Pereverzev and et al.: Diamond and Related Materials, vol. 4 (1995), p. 754
- [14] M. Wieligor and T. W. Zerda: Diamond and Related Materials, vol. 17 (2008), p. 84